



Article

Reprocessability of PLA through Chain Extension for Fused Filament Fabrication

Carlos Correia ¹, Tiago E. P. Gomes ¹, Idalina Gonçalves ² and Victor Neto ^{1,*}

¹ Centre for Mechanical Technology and Automation, Department of Mechanical Engineering, University of Aveiro, 3810-193 Aveiro, Portugal; carlos.correia@ua.pt (C.C.); tiago.emanuel.gomes@ua.pt (T.E.P.G.)

² CICECO—Aveiro Institute of Materials, Department of Materials and Ceramic Engineering, University of Aveiro, 3810-193 Aveiro, Portugal; idalina@ua.pt

* Correspondence: vneto@ua.pt

Abstract: As additive manufacturing (AM) technologies have been gaining popularity in the plastic processing sector, it has become a major concern to establish closed-loop recycling strategies to maximize the value of the materials processed, therefore enhancing their sustainability. However, there are challenges to overcome related to the performance of recycled materials since, after mechanical recycling, the molecular degradation of thermoplastics shifts their performance and processability. In this work, it was hypothesized that the incorporation of a chain extender (CE) during the reprocessing would allow us to overcome these drawbacks. To attest this conjecture, the influence of 1,3-Bis(4,5-dihydro-2-oxazolyl)benzene (PBO), used as a CE, on mechanical, thermal, and rheological properties of polylactic acid (PLA) was studied. Furthermore, a closed-loop recycling system based on Fused Filament Fabrication (FFF) was attempted, consisting of the material preparation, filament extrusion, production of 3D components, and mechanical recycling steps. PBO partially recovered the recycled PLA mechanical performance, reflected by an increase in both tensile modulus (+13%) and tensile strength (+121%), when compared with recycled PLA without PBO. Printability tests were conducted, with the material's brittle behavior being the major constraint for successfully establishing a closed-loop recycling scheme for FFF applications.

Keywords: additive manufacturing; PLA; plastic recycling; PLA chain extension; PBO; thermo-mechanical degradation



Citation: Correia, C.; Gomes, T.E.P.; Gonçalves, I.; Neto, V. Reprocessability of PLA through Chain Extension for Fused Filament Fabrication. *J. Manuf. Mater. Process.* **2022**, *6*, 26. <https://doi.org/10.3390/jmmp6010026>

Academic Editor: Joshua M. Pearce

Received: 7 December 2021

Accepted: 14 February 2022

Published: 19 February 2022

Publisher's Note: MDPI stays neutral with regard to jurisdictional claims in published maps and institutional affiliations.



Copyright: © 2022 by the authors. Licensee MDPI, Basel, Switzerland. This article is an open access article distributed under the terms and conditions of the Creative Commons Attribution (CC BY) license (<https://creativecommons.org/licenses/by/4.0/>).

1. Introduction

The pathway into the future will require a smarter management of both materials and energy in order to reach a sustainable usage of the planet's limited resources. In this context, waste management, plastic recycling in particular, constitutes one of the most important and interesting challenges for achieving a sustainable society. Although plastics were only introduced in large-scale production in the mid-twentieth century, their versatile properties and easy processing has led them to be prime materials with a wide range of applications [1]. However, their dependency on fossil feedstocks and improper disposal leads to their accumulation on land and marine environments, which brings a negative impact on natural ecosystems, thus being a subject of great concern from social, academic, and governmental perspectives [1].

As an alternative to the petroleum-sourced plastics, bio-based and biodegradable polymers, such as polylactic acid (PLA), have been receiving much attention since they can be produced from renewable sources and provide a composting-based end-of-life disposal pathway [2]. Nonetheless, several authors state that the application of compostable polymers in single-use commodities is unsustainable, and hence their recyclability should be addressed in order to ensure extended value for these materials [2,3]. Reprocessing the plastics by multiple extrusion or injection molding has been a common approach to assess the

recyclability of polymers and to study the thermomechanical degradation during processing and mechanical recycling [4]. Pillin et al. addressed the reprocessability of poly(L-lactic acid) (PLLA) for up to seven reprocessing cycles, using multiple-injection molding with constant injection parameters, monitoring the evolution of rheological, thermal, and mechanical properties and reported an increase in PLLA crystallization and a severe depletion of the tensile properties as a function of the processing cycles explained by the strong degradation of the polymer during reprocessing, yielding large chain scission evidenced by rheological experiments and molecular weight measurements [5]. Zenkiewicz et al. studied the rheological, thermal, and mechanical changes for up to 10 reprocessing cycles using the successive extrusion of PLA, and reported a depletion of tensile properties and impact strength, a slight decrease in its thermal stability and a significant increase in PLA melt flow rate as a function of the extrusion number [6]. However, the author states that PLA regrinding could yield new additives to the neat polymer [6]. Sanchez et al. analyzed the recyclability of PLA for up to five reprocessing cycles using FFF technology and micro-injection molding, and monitored the degradation that occurred during the mechanical recycling [7]. In this study, it was reported that, although it was feasible to use recycled PLA for an open-source AM, the decrease in the tensile properties induced by the 3D-printing manufacturing cycle indicate that the material cannot be recycled as many times as in the injection molding process [7].

A mechanical recycling-based system is composed of the processes of sorting, washing, grinding, and re-compounding of the plastic waste in order to provide feedstock for further (re)processing and can be applied either to post-industrial (PI) or post-consumer (PC) plastic waste streams in closed-loop or open-loop recycling schemes [8]. The main challenge for introducing recycled feedstocks in the plastic manufacturing cycle is related to the degree of mixing with different chemical classes of plastic polymers and other contaminants (particularly when handling complex mixtures from post-consumer waste streams) and their degree of degradation caused by the processing and service life [4]. Polymers are prone to degrading due to the processing and environmental conditions that they are exposed, decreasing their molecular weight [5,9–11] and performance, as reflected on their mechanical [5,9], rheological [6,7] and thermal properties [12–14].

Currently, different strategies for upgrading degraded polymers have been addressed, particularly polymer restabilization; copolymerization; incorporation of a certain percentage of virgin polymers together with the recycled feedstocks; and rebuilding of the cleaved molecular chains [2–4]. The rebuilding of degraded polymers through the application of functional additives, such as chain extenders (CE), has been proved to be an interesting approach for enhancing the properties of recycled PLA [2]. In particular, the incorporation of functional CE into PLA-based materials favors the reaction between the PLA carboxyl and hydroxyl groups and can either be applied directly through reactive extrusion or by employing an additional melt-mixing stage [15,16]. Several authors have addressed the possibility of rebuilding degraded PLA through multifunctional CE, particularly epoxy-based CE, such as Joncryl ADR 4368, reporting improvements on the material's molecular weight and molecular weight distribution without sacrificing its mechanical and thermal performance [17]. Meng et al. studied the influence of phosphite-based CE on the performance of PLA, reporting a significant improvement of the recycled PLA toughening properties [18,19], whereas Han et al. addressed the possibility of using functional polysilsesquioxane (FPSQ), which has no detrimental influence on the environmentally friendly properties of PLA, to increase the polymer's melt strength [20]. Herrera et al. studied the effect of different CE in distinct polymerization stages, particularly 1,3-phenylene-bis-2-oxazoline (PBO) and 1,10-carbonyl bis caprolactam (CBC), showing that PLA-CE systems were less sensitive to degradation than the neat PLA [21]. In this context, rebuilding degraded polymer chains through chain extension favors the formulation of a polymer with restored molecular weight and stable properties that can possibly fulfill the rheological requirements of a wide range of polymer processing techniques [22], including AM technologies [23,24].

Additive Manufacturing (AM) is the general term for a group of technologies which are based on the creation of 3D objects by the successive addition of a material, in opposition to the conventional subtractive manufacturing technologies such as machining, where a 3D part is created by subtracting material from a solid block [25]. Within AM, Material Extrusion (MEX), often designated as Fused Deposition Modeling (FDM) or Fused Filament Fabrication (FFF), is a process in which the material is selectively deposited through a nozzle to create 3D parts in a layer-by-layer methodology and represents the most widely spread AM-related technology available for both industrial and consumer–manufacturer applications [25–27]. The feedstocks generally used in FFF are thermoplastics, such as acrylonitrile butadiene styrene (ABS) and PLA, in the shape of a thin filament with a diameter of 1.75 mm or 2.85 mm [27]. In particular, PLA has been the material of choice for most FFF-based applications, since it has a low melting temperature and it is of easy processing. Moreover, several commercial filament manufacturers are already moving towards a recycled polymer-based production, such as RE-PET3D [28], Filamentive [29], Reflow [30], and Tucab [31], which offer filaments made by recycled PLA and polyethyl benzene-1,4-dicarboxylate (PET), in order to promote sustainability among the consumers and enthusiasts. Additionally, the development of desktop-range filament extruders provides the opportunity for the extended recycling of AM by-products as well as the research and development of new recycling procedures. In this context, based on the knowledge of both material science and processing equipment areas, it is possible to establish circular and sustainable value chains, such as the distributed recycling via an additive manufacturing (DRAM) waste management strategy [32,33]. Moreno et al. reported that DRAM can contribute to the development of a more circular economy, as it provides a feasible valorization pathway for recycled PLA, from a material properties perspective [34]. However, the source and composition of the waste streams is highlighted as a constraint, since heterogeneity and degradation of the materials can lead to poor performance [34]. Grigora et al. addressed the possibility of upgrading PLA for injection molding applications to be employed in AM, through the incorporation of a functional chain extender, decreasing the melt flow rate of the material and achieving filaments of improved quality and 3D-printed parts with enhanced tensile properties [35]. In this context, the goal of this study was to attest to the valorization of recycled PLA from injection molding waste streams through a DRAM-enabled pathway, which could contribute to enhanced sustainability of production, in accordance with the circular manufacturing principles. Furthermore, the incorporation of a fixed amount (1%) of PBO, a functional additive that was successfully employed by Herrera et al. as an effective chain extender for PLA-based materials, in the virgin and recycled feedstocks was incorporated, in order to understand to what extent the rebuilding of the degraded polymeric chains could help to recover the PLA-based material properties, therefore providing a pathway for the production of functional components with recycled PLA. To achieve these objectives, the influence of PBO and multiple cycles on the structure, mechanical, and thermal properties of an industrial-grade PLA designed for injection molding applications was addressed, and the possibility of establishing a closed-loop recycling network based on the proposed valorization pathway was postulated.

2. Materials and Methods

2.1. Materials

An industrial-grade PLA, ErcrosBio[®] LL 602, produced by Ercros (Barcelona, Spain) and supplied by AGI (Vila Nova de Gaia, Portugal) was selected for addressing an FFF-based multi-processing approach. According to the manufacturer's specifications, this grade of PLA is primarily intended for injection molding applications. From its technical data sheet (TDS), it is known that the material has a density of 1.25 g/cm³, tensile modulus of 3000 MPa, tensile strength of 68 MPa, tensile elongation of 3%, a glass transition temperature of 63 °C, and a MFI of 17 g/10 min, measured at 195 °C and 2.16 kg load. Prior to the processing steps, the PLA-based material was dried in a convection oven at 60 °C for 9 h and cooled at ambient conditions in order to stabilize its moisture content.

1,3-Bis(4,5-dihydro-2-oxazolyl)benzene (PBO) supplied by TCI Chemicals (Zwijndrecht, Belgium). This is a powdered component with a weight-average molecular weight of 216.24 g/mol and melting temperature between 146 °C to 149 °C.

2.2. Methods

Four different recycling chains, Figure 1, composed by the material preparation, filament extrusion, fabrication of 3D samples, evaluation of properties, and plastic recycling, were employed in order to access the recyclability of PLA and the recovery of its properties via the addition of PBO. The first recycling process chain was based on the neat PLA and will be referred hereafter as vPLA. A second recycling chain based on recycled PLA obtained through a mechanical recycling simulation encompassed by the processes of drying, filament extrusion, and 3D printing was considered as a reference for the behavior of the recycled material and will be designated hereafter as rPLA. The remaining recycling process chains were obtained by the compatibilization of the neat and recycled polymer with PBO and will be referred as vPLA+PBO and rPLA+PBO. The CE content was fixed on 1% *w/w* based on the knowledge gathered from previous works involving the upgrading strategies for recycled PLA [21].

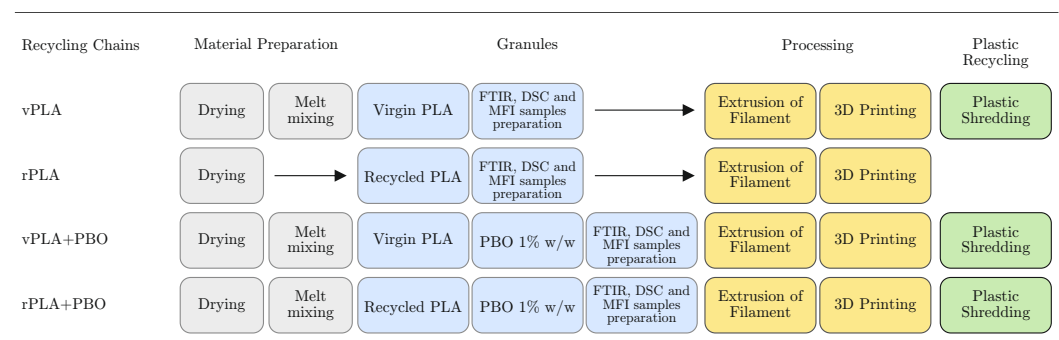


Figure 1. Description of the four different recycling chains and the processes involved (adapted from [7]).

2.3. Extrusion of PLA-Based Monofilaments

Before the filament extrusion stage, and in order to obtain a homogeneous mixture between the PLA and the CE, a laboratory-scale mechanical melt-mixing process was employed by using a Plastograph EC Brabender (BRABENDER GMBH & CO. KG, Duisburg, Germany) torque rheometer. All the formulations (including the virgin PLA) were subjected to the melt mixing stage in order to normalize (i.e., bypass) the degradation associated with this additional processing step, which was assumed to be similar for all the different formulations. For each batch, 250 g of PLA were considered, and for the compatibilized formulations 2.5 g of PBO was added after the complete melting of the polymer in order to fulfill the desired CE concentration. The mixing conditions were set according to the material melt behavior. In this context, the equipment temperature was set up to 180 °C, the speed to 75 rpm and the residence time from 5 to 10 min. In particular, the residence time was defined according to the time required to the torque to stabilize. However, different formulations required equally different residence times, probably due to the shape factor of the recycled PLA flakes. In this context, 10 min was established as the maximum residence time, in order to prevent excessive degradation of the material, according to the experiments conducted by Marec et al. [36]. After the blending stage, the obtained mixtures were grinded to ≈ 6 mm flakes on the same equipment that was employed in the plastic shredding stage, to allow them to be fed to the filament extruder.

The extrusion of monofilament was conducted on a Next 1.0 Advanced (3DEVO, Utrecht, Netherlands) desktop filament extruder, equipped with an in-line diameter sensor and an automated winding system. The temperature profile employed, from the die to the feeding zone was 180 °C, 175 °C, 170 °C, 165 °C and the screw speed was set up to 4 rpm.

The success criterion for the production of monofilament was the diameter consistency which was set within a range between 1.65 mm and 1.85 mm, with 1.75 mm as the diameter sensor target.

2.4. Printability of the PLA-Based Filament

The selected FFF machine was a Ender-3 (CREALITY, Shenzhen, China), an open-source cartesian 3D printer, equipped with a Bowden tube-based extruder and which has been the equipment of choice for many hobbyists and consumer-manufacturers since it represents a low initial investment and has a large online support community. Prior to the machine operation, the digital models were developed through the educational version of SOLIWORKS 2020 CAD software, converted to a STL file and pre-processed through ULTIMAKER CURA 4.9.1 slicing software. The process parameters, which were crafted according to the part specifications and material melt behavior, are presented in Table 1.

Table 1. Process parameters used for the fabrication of the printed samples (adapted from [7]).

	Dumbbell (ISO 527-02, Type 1BA)	Regular Dodecahedron
Toolpaths	90°–90°	90°–0°
Layer height	0.1 mm	0.2 mm
Bed temperature	60 °C	60 °C
Extruder temperature	190 °C	190 °C
Wall line count	2	2
Top layers	4	4
Bottom layers	4	4
Infill density	100%	15%
Travel speed	150 mm/s	200 mm/s
Nozzle diameter	0.4 mm	0.4 mm
Raster width	0.5 mm	0.48 mm
Print speed	40 mm/s	80 mm/s
G-code	Ultimaker Cura 4.9.1	Ultimaker Cura 4.9.1

2.5. Mechanical Recycling of PLA-Based Materials

The plastic shredding stage of PLA-based 3D-printed parts was conducted on a Wanner C 13.20S plastic granulator (WANNER TECKNIK GMBH, Wertheim, Germany) equipped with a 6 mm sieving unit. According to the manufacturer, this equipment was designed in order to reduce friction on the cutting chamber, preventing the warming up of the blades and, therefore, limiting the rate of thermo-mechanical degradation on the regrind [37].

2.6. Characterization of the PLA- and PLA/PBO-Based Materials

2.6.1. Linear Mass Density and Extrusion Rate

The linear mass density (μ) of the filament was calculated from the ratio between the filament weight and the filament length by following Equation (1). The theoretical linear mass density (μ_t) was determined through the polymer's density as stated in the manufacturer TDS and the filament average cross-sectional area as seen in Equation (2).

$$\mu = \frac{\text{Filament weight}}{\text{Filament length}} \quad [\text{g/m}] \quad (1)$$

where μ represents the linear mass density in g/m. The filament weight (g) was measured after extrusion on an analytical balance, and the filament length (m) was obtained through the extruder's data acquisition software.

$$\mu_t = d \cdot A_c \quad [\text{g/m}] \quad (2)$$

where μ_t represents the theoretical linear mass density in g/m, d the density in g/cm³ and A_c the filament cross-sectional area in mm².

Moreover, and, since the process parameters for the extrusion stage were kept constants for all formulations, the evolution of the extrusion rate was calculated by following Equation (3).

$$\text{Extrusion rate} = \frac{\text{Filament length}}{\text{Extrusion time}} \quad [\text{m/min}] \quad (3)$$

where *Filament length* (m) and *Extrusion time* (min) were obtained through the extruder's data acquisition software.

2.6.2. Tensile Tests

Random segments of PLA-based filaments were selected for accessing the material mechanical behavior following the standard test for determining the tensile properties of single-filament materials (ASTM D3379). In this context, a cardboard mounting tab similar to the one presented in Figure 2 was developed in order to decrease the clamping breaks, which lead to the failure of the test. The filament test specimens have a gage length of 60 mm and were fixed to the mounting tab by means of a hot glue bead. The tensile tests were achieved by means of a TA.XT Plus C texture analyzer (STABLE MICRO SYSTEMS, Godalming, UK) equipped with a micro-tensile grip. For all the samples, the selected loading speed was 1 mm/s and a 0.3 kN load cell was used.

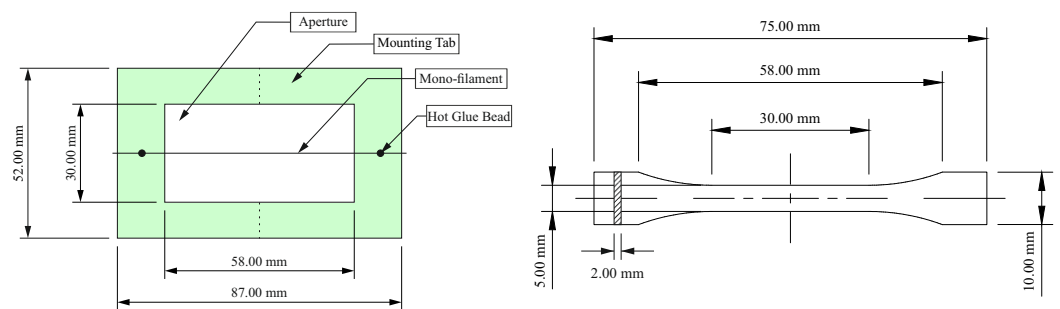


Figure 2. Representation of the mounting tab for single-filament tensile tests (According to [38]—left) and technical specifications for the ISO 527-02 Type 1BA dumbbell tensile test specimen (According to [39]—right).

Moreover, dumbbell-shaped test specimens (ISO 527-02, Type 1BA) were produced, in order to access the tensile properties of the PLA-based materials after being processed through FFF technology. The test specimens were prepared and produced according to the procedure described in Section 2.4. The tensile tests were conducted on a universal tensile testing machine AUTOGRAPH AGS-X SERIES (Shimadzu, Kyoto, Japan). At least four replicates were tested, at a loading speed of 1 mm/min, and a 50 kN load cell was employed.

2.6.3. Surface Morphology

Small segments of filament were broken after being exposed to $-70\text{ }^{\circ}\text{C}$ for ≈ 15 min in order to obtain a clean cross-section for the SEM analysis. The images were collected using a scanning electron microscope TM4000Plus (HITACHI, Tokyo, Japan), operated at 10 kV. Carbon conductive tape was applied to the sample holder before analysis to avoid charging. The images were recorded in the magnification range of $\times 500$ to $\times 1000$ at different locations on the surface.

2.6.4. Chromatic Measurements

The chromatic properties were evaluated using a portable colorimeter Chroma Meter CR-400 (KONIKA MINOLTA SENSING, INC., Tokyo, Japan), calibrated with a white standard tile. The color coordinates L^* , a^* , and b^* were collected, where L^* stands for the luminance or the prevalence between black and white, a^* indicates the change from green to

red, and b^* represents the change between blue and yellow [14,40]. The color measurements required the conformation of thin flat film which was obtained by means of a hot plate press at the temperature of 200 °C and a pressure around 100 bar for 1 min. At least five replicates were obtained for each sample and the corresponding average values and standard deviations were calculated. The total difference in color (ΔE^*_{ab}) was calculated according to Equation (4).

$$\Delta E^*_{ab} = \sqrt{(\Delta L^*)^2 + (\Delta a^*)^2 + (\Delta b^*)^2} \quad (4)$$

where ΔL^* , Δa^* , and Δb^* are the L^* , a^* , and b^* differences between each sample and the vPLA [40].

The color change was reported by addressing the following criteria: unnoticeable difference ($\Delta E^*_{ab} < 1$), slight difference ($1 \leq \Delta E^*_{ab} < 2$), noticeable difference ($2 \leq \Delta E^*_{ab} < 3.5$), evident difference ($3.5 \leq \Delta E^*_{ab} < 5$) and different colors ($\Delta E^*_{ab} \geq 5$) [14].

The yellowness index was obtained from the CIE color space values and the ASTM E313 method by considering an illuminant D65 and a standard observer function of 10°, following Equation (5) [14].

$$YI = \frac{100(1.3013X - 1.1498Z)}{Y} \quad (5)$$

2.6.5. Differential Scanning Calorimetry (DSC)

DSC tests were conducted on a NexTA STA300 heat-flux calorimeter (HITACHI, Tokyo, Japan) using Linseis TA Evaluation software for data collection and treatment. Samples with weights between 5 mg and 10 mg were sealed in aluminum pans according to the sample preparation procedure described by the ISO 11357-1 standard. The samples were subjected to two heating steps, with the first heating schedule starting from 25 °C to 120 °C and kept at 120 °C for 10 min. The second heating schedule started from 30 °C to 250 °C. An intermediate cooling step was also employed, starting from 120 °C to 30 °C and including a 10 min standby. All of the heating and cooling steps were conducted at a rate of 10 °C/min.

The main objective of the first heating scan was to eliminate the heat history of the samples; therefore, all the transition temperatures including the cold crystallization temperature (T_{cc}) and melting temperature (T_m), as well as cold crystallization (ΔH_{cc}) and melting (ΔH_m) enthalpies were recorded from the second heating sequence according to the procedures highlighted in the ISO 11357 standard [41].

Moreover, based on the melting enthalpy, known to be directly proportional to the crystallinity of a polymer, the crystallinity ratio or degree of crystallinity (χ) of each sample was determined by following Equation (6).

$$\chi(\%) = \frac{\Delta H_m - \Delta H_{cc}}{\Delta H_{\infty}} \quad (6)$$

where ΔH_m and ΔH_{cc} (J/g of polymer) are the melting enthalpy and the cold crystallization enthalpy, respectively. ΔH_{∞} is 93.1 J/g, which is the melting enthalpy for a 100% crystalline PLA [42].

2.6.6. FTIR Spectroscopy

Infrared spectra of the films that were used in the context of the color measurement analysis were obtained with a Bruker compact FTIR spectrometer, model ALPHA (BRUKER CORPORATION, Billerica, MA, USA), using a PLATINUM attenuated total reflection (ATR) module on absorbance mode. First, a background spectrum was recorded and subtracted from the sample spectra in the area from 4000 cm^{-1} to 600 cm^{-1} . The number of scans was 32, with a wavelength resolution of 4 cm^{-1} . In order to assure accurate results, at least five replicates were conducted for each sample. Data collection was performed on the equipment's proprietary software OPUS 7.0 and exported to a custom Excel datasheet.

2.6.7. Melt Flow Rate (MFR)

The measure of the MFR was conducted through a semi-automatic melt flow indexer MI-3 (GÖTTFERT, Buchen, Germany), which determines the melt flow rate based on ISO 1133 Procedure A test standard. Following the manufacturer specifications test conditions (195 °C/2.16 kg), the polymer presented such a high fluidity that the test was impossible to conduct. In this context, several conditions were tested with temperatures ranging from 190 °C to 170 °C and a constant load of 2.16 kg. With the temperatures above 180 °C, the fluidity was still too high for correctly employing the test procedure, however with temperatures below 180 °C the material did not completely melt, and the test results were discarded. The load was then reduced to 1.2 kg and the temperature set at 180 °C. At least three replicates were performed, each of those employing around 10 g of material through a Ø2.095 mm standard die.

2.6.8. Printability Assessment

A qualitative approach for determining the 3D-printing capacity of the material, either on its virgin, recycled, and compatibilized counterpart was conducted on a regular dodecahedron printed component, following an established criteria which includes the success of the print, and a visual inspection for defects, such as the presence of voids under or over-extrusion, and layer shifts. This component was prepared and produced according to the procedure described in Section 2.4.

2.7. Statistical Analysis

The characterization data were statistically analyzed through analysis of variance. Microsoft Excel custom sheet was used as the data treatment software.

3. Results and Discussion

3.1. Extrusion of PLA-Based Filaments

The filament production rate data highlight that, for all the formulations developed, filaments with a consistent diameter, within the processable range for a general FFF machine, were obtained (Table 2). However, the high fluidity of pristine PLA, together with the inefficient cooling of the filament extruder, contributed to the production of a brittle filament, which undermined the further processing stages.

From the analysis of the linear mass density consistency (Figure 3), it was possible to identify the presence of inclusions, such as air bubbles or other contaminants, entrapped within the filament. In this context, vPLA presented a deviation between μ and μ_t of 31%. On the other hand, vPLA+PBO and rPLA+PBO, presented a deviation between μ and μ_t of 12% and 14%, respectively. These results demonstrate that the virgin PLA was the most dopped formulation. There was no evidence of what kind of inclusions were present in the virgin PLA formulation, and, therefore, they were assumed to be related to the presence of additives that were incorporated into the supplied PLA (e.g., antioxidants) during the melt-mixing stage, as it was the most exposed processing stage due to the lack of a protective atmosphere. Further processing stages were responsible to minimize the inclusions, possibly caused by the molecular chains reorganization, and, therefore, are assumed to be the reason for their absence in the recycled PLA formulations.

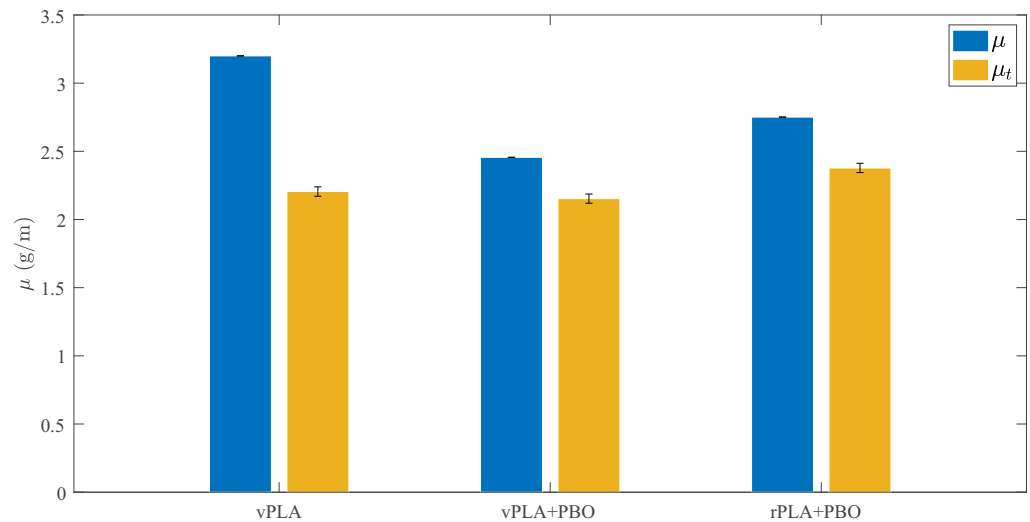


Figure 3. Linear mass density of the filament produced with virgin PLA (vPLA), virgin PLA mixed in the presence of PBO (vPLA+PBO), and recycled PLA mixed in the presence of PBO (rPLA+PBO).

Table 2. Characteristics of the filament produced with the virgin PLA (vPLA), recycled PLA (rPLA), virgin PLA mixed in the presence of PBO (vPLA+PBO), and recycled PLA mixed in the presence of PBO (rPLA+PBO).

	Average Diameter (mm)	Filament Length (m)	Extrusion Rate (m/s)
vPLA	1.764 ± 0.598	52.094	1.27
rPLA	1.702 ± 0.870 (*)	-	-
vPLA+PBO	1.722 ± 0.221	62.363	1.39
rPLA+PBO	1.740 ± 0.146	62.294	1.67

* Filament average diameter was extrapolated from manual measurements and presented for the sake of comparison.

The quantity of filament produced, reflected by the output filament length, indicated that filament extrusion does not represent an excessive waste of material, even when handling with 100% recycled polymer. For the filament produced with rPLA, the output filament length, extrusion rate, and, consequently, the linear mass density were unable to be monitored due to an error in the data acquisition software. However, the filament average diameter was extrapolated from manual measurements and presented for sake of comparison. Computing the filament length of the recycled PLA formulation by using an external device was unable to be conducted as the re-spooling of the filament was impossible to render due to the extreme brittleness of the material. The evolution of the extrusion rate presents an increasing trend, particularly between the vPLA and rPLA+PBO formulations, which may anticipate a decrease in melt strength, which will be accessed with further testing.

3.2. Filament Tensile Performance

The results from the filament tensile tests (Figure 4) illustrates that the vPLA filament tensile strength is substantially lower than the reported ones [43,44]. This behavior is translated by a decrease in both tensile strength (−83.38%) and elongation at break (−61.70%) of vPLA filaments, when compared to the PLA control material used by Petchwattana et al. and can be explained by the effect of the melt-mixing and grinding steps. These additional processing steps were employed to the virgin polymer in order to normalize the degradation caused by these material preparation stages, therefore allowing us to achieve comparable data about the extent of degradation between the pristine materials and the compatibilization of the PLA-based materials and the CE.

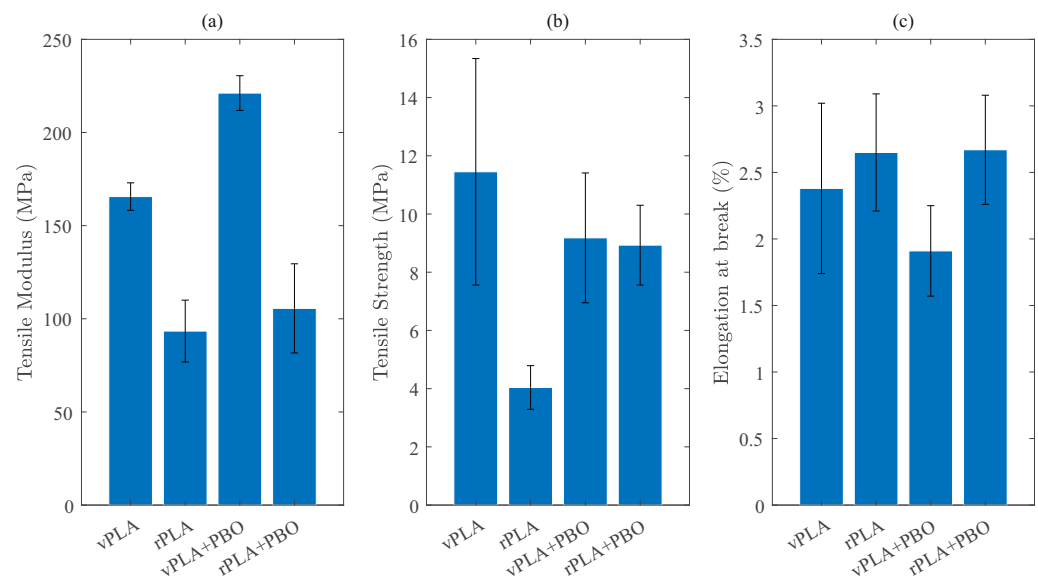


Figure 4. Tensile modulus (a), Tensile Strength (b), and Elongation at break (c) of the filament produced with the virgin PLA (vPLA), recycled PLA (rPLA), virgin PLA mixed in the presence of PBO (vPLA+PBO), and recycled PLA mixed in the presence of PBO (rPLA+PBO).

After chain extension, the virgin PLA exhibited an increase in tensile modulus (+33.5%), as well as a decrease in both ultimate tensile strength (−19.8%) and elongation at break (19.7%), when compared to vPLA. These results suggest that the incorporation of PBO into the pristine PLA had a negative impact on its ultimate tensile properties, a behavior which can be associated with a low interaction between vPLA and the CE, as previously reported by Herrera et al. [21].

Recycled PLA (rPLA) presented a substantial decrease in tensile modulus (−43.60%) and tensile strength (−64.72%). However, the elongation at break exhibited a slight increase of ≈10%, when compared to the pristine material. In the presence of PBO, the recycled polymer partially recovers its tensile properties, as observed by the increases in both tensile modulus (+13%) and tensile strength (+121%), when compared with rPLA.

Figure 5 presents the stress–strain curves for all the formulations of each recycling chain that highlight the fragile behavior of the material demonstrated by the absence of plastic deformation. The brittle nature of this grade of PLA represents the major constrain for the development of a multi-processing approach based on FFF, since the feedstock material for this technology has to be flexible enough in order to be continuously pushed by the machine towards the print head [45]. Moreover, the tendency for the recovery of the tensile properties after chain extension is evident in the rPLA+PBO curve, which is in agreement with several reports from the literature [23,46,47].

3.3. Morphology

3.3.1. Surface Morphology

The smooth surface of the neat PLA (Figure 6a) suggests a brittle fracture of the material, corroborating with the literature [43], which was, in fact, confirmed by the filament tensile tests. Moreover, the white areas highlighted on the micrographs may represent some kind of inclusions that were trapped into the polymer matrix during processing, a behavior also reported by Brüster et al when analyzing plasticized PLA-based formulations [9] and which is in agreement with data from the linear mass density consistency analysis.

In the presence of PBO, (Figure 6b) the smooth surface was covered in peninsula-like layers and short uneven fibrils which are speculated to be a result of the reaction between the polymer and PBO, in agreement with the observations conducted by Tuna et al. on the fracture morphology of PLA/CE matrices [15]. Regarding the use of both recycled PLA and PBO, the formulation's microstructure presented a rougher and more

heterogeneous surface than the pristine PLA-based materials, an observation which is in agreement with the reports by Badia et al. [12] and may be related to the decrease in mechanical performance, a hypothesis which was confirmed by the filament tensile tests.

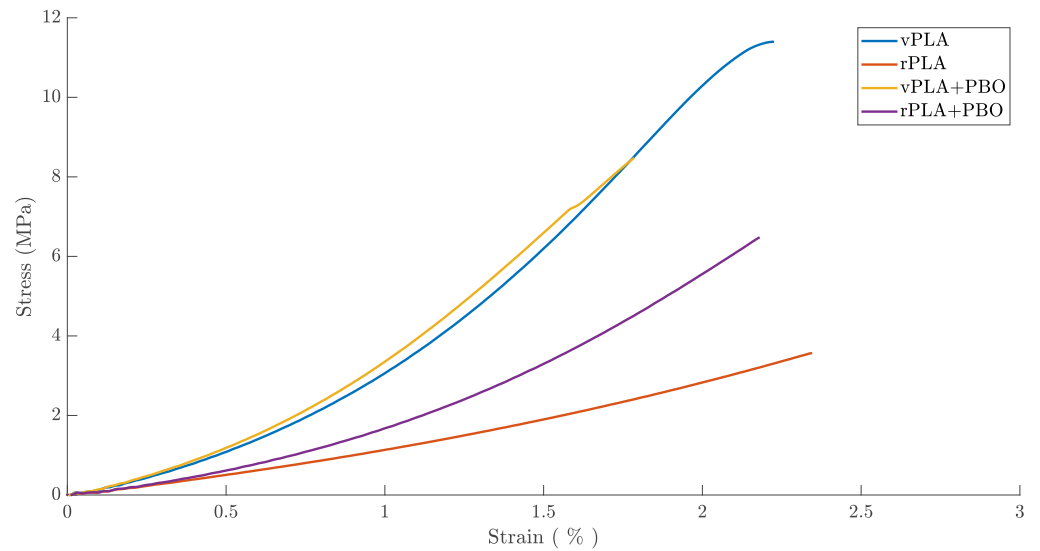
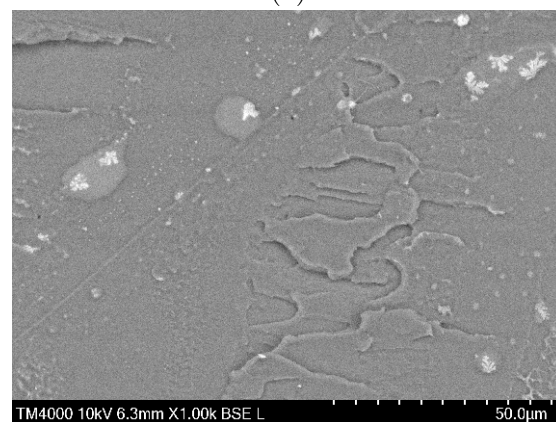


Figure 5. Stress–strain curves for virgin PLA (vPLA), recycled PLA (rPLA), virgin PLA mixed in the presence of PBO (vPLA+PBO), and recycled PLA mixed in the presence of PBO (rPLA+PBO), highlighting the recovery of the mechanical properties of rPLA after chain extension.

(a)



(b)

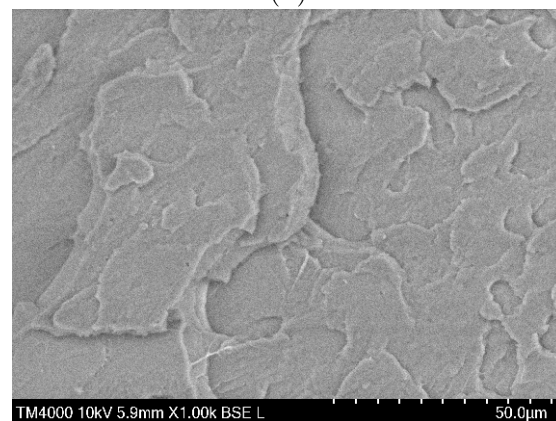


Figure 6. Cont.

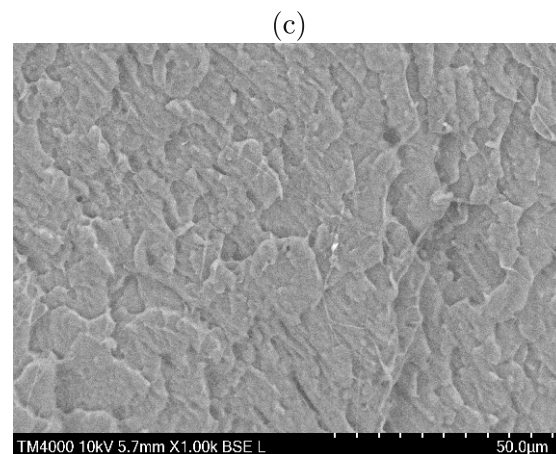


Figure 6. SEM micrographs representing the cross-sectional microstructure of the filament produced with (a) vPLA; (b) vPLA+PBO; (c) rPLA+PBO at a magnification of $\times 500$.

3.3.2. Optical Measurements

The incorporation of PBO on either virgin or recycled PLA did not significantly change the average luminosity of the samples, with the highest L^* value being observed for the rPLA+PBO sample (Table 3). On the other hand, a^* (red-green) and b^* (blue-yellow) color coordinates significantly change for the modified formulations, particularly the b^* color coordinate which represents a yellowing tendency of the polymer after the PBO incorporation, enhanced for the recycled PLA-based blend. The tendency for PLA discoloration after melt processing has been described in the literature as a problem which adversely affects the properties and end use of the final products [48]. On the studied formulations, the yellowing was detected even in the control materials, which suggests that the color modifications may have resulted from some oxidation that occurred during the melt-mixing stage. When in contact with the atmosphere, free radicals from the polymer's cleaved chains react with the oxygen to form new molecules, which, in turn, will absorb and reflect different wavelengths, therefore leading to variations in color. Since reprocessed PLA is expected to have more cleaved chains available to react with the oxygen, this effect will be higher for recycled PLA-based materials, a behavior which is reflected by the evolution of the yellowness index, a standard parameter which describes the change in color from white towards yellow, and that was previously documented by Agüero et al. and Carrasco et al. [14,49]. The total difference in color measured by ΔE_{ab^*} shows a noticeable variation in color in vPLA+PBO and rPLA+PBO formulations, when compared to the neat PLA.

Table 3. Average numbers for luminance (L^*), green-red (a^*), blue-yellow (b^*), total color difference (ΔE_{ab^*}) and yellowness index (YI) for virgin PLA (vPLA), virgin PLA mixed in the presence of PBO (vPLA+PBO), and recycled PLA mixed in the presence of PBO (rPLA+PBO).

	L^*	a^*	b^*	ΔE_{ab^*}	YI
vPLA	84.682 ± 0.921	0.556 ± 0.037	1.134 ± 0.160	-	32.915
vPLA+PBO	83.348 ± 0.957	0.090 ± 0.051	4.200 ± 0.400	3.376	37.415
rPLA+PBO	85.044 ± 0.854	0.266 ± 0.008	4.432 ± 0.464	3.330	37.858

3.4. Thermal Behavior

The thermograms of the PLA-based formulations (Figure 7; Table 4) showed the presence of a first endothermic peak between 155°C and 159°C related to the PLA crystallization. Further, a single melting peak appeared in the temperature range between 173°C and 175°C . On the other hand, the neat PBO thermogram showed the presence of an endothermic peak around 148°C associated with its melting phase transition. From these results, an insignificant variation in the glass transition temperature between the virgin PLA and the compatibilized formulations was noticed, which is in agreement with

several reports from the literature (see [9,10,49]). Similarly, the cold crystallization temperature (T_{cc}) did not significantly change, with exception of the rPLA+PBO formulation, which presented a slight decrease in T_{cc} when compared to the virgin polymer counterpart. The determined melting temperature of vPLA was inferior to the one mentioned in the manufacturer's TDS. This behavior may be explained by the material preparation stages, particularly the melt-mixing and grinding operations which were performed in order to normalize the degradation degree between the virgin PLA and compatibilized formulations. However, among all the studied samples, the melting transition did not significantly change, which allowed for the material to be processed at constant conditions.

Table 4. Thermal properties determined from the DSC thermograms for virgin PLA (vPLA), virgin PLA mixed in the presence of PBO (vPLA+PBO), and recycled PLA mixed in the presence of PBO (rPLA+PBO).

	T_g (°C)	T_{cc} (°C)	T_m (°C)	X (%)
vPLA	64.5	158.4	174.1	35.77
vPLA+PBO	66.2	159.1	175.0	24.28
rPLA+PBO	64	155.8	173.7	32.79
PBO	-	-	147.9	-

From the analysis of the crystallization degree (Figure 8), it was inferred that the amorphous domains tended to prevail more in the PLA formulations than the crystalline ones [21] and PBO decreased the PLA crystallinity. This particular observation suggests that PBO led to a more restrict mobility of the polymeric chain which, in turn, is unfavorable to the formation of orderly crystalline structures within the polymeric chains [46]. In contrast, an opposite result was expected for the recycled polymer, since the cleavage of the polymeric chains due to the chain scission phenomena would promote a higher mobility of these structures and, therefore, the formation of crystalline domains. In this context, the slight decrease in the degree of crystallinity between vPLA and rPLA+PBO may be an indicator of an effective chain extension, although further testing would be required to validate this hypothesis.

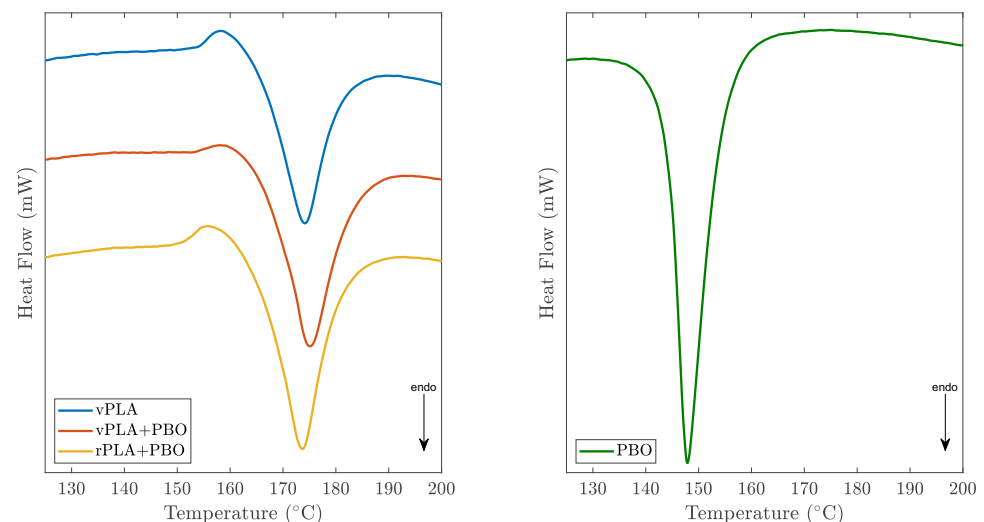


Figure 7. DSC thermograms recorded during the second heating of samples: PLA formulations (**left**); neat chain extender (**right**).

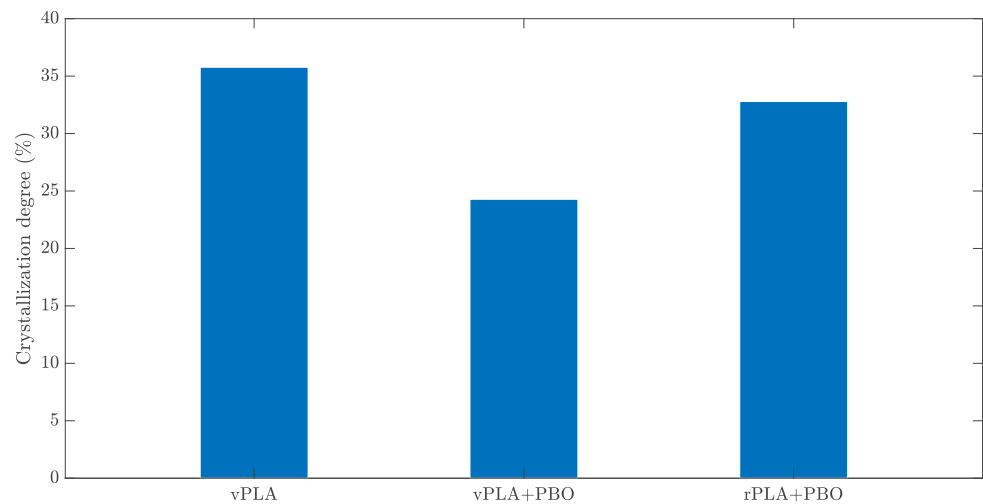


Figure 8. Representation of the crystallization degree for virgin PLA (vPLA), virgin PLA mixed in the presence of PBO (vPLA+PBO), and recycled PLA mixed in the presence of PBO (rPLA+PBO).

3.5. Structural Analysis

By comparing the obtained FTIR spectra (Figure 9), the absence of modifications in the characteristic wavenumbers for PLA, particularly around 1745 cm^{-1} related to the presence of carbonyl groups (C=O), CH_3 deformation vibration at 1450 cm^{-1} , and C-O stretching at 1180 cm^{-1} and 1078 cm^{-1} , suggests a low interaction established between the PLA and PBO. Similar results were previously reported by Herrera et al. for this PBO concentration [21]. This behavior may be explained either by the CE's functionality, since PBO acts as a di-functional chain extender, with two reactive sites, and, therefore, a higher concentration should be accounted for promoting chain extension, or by the limited structural degradation of the formulation after processing (for virgin PLA-based materials) and reprocessing (for recycled PLA-based materials), which, although reflected by a decrease in mechanical performance, can be insufficient to promote effective reaction with the PBO.

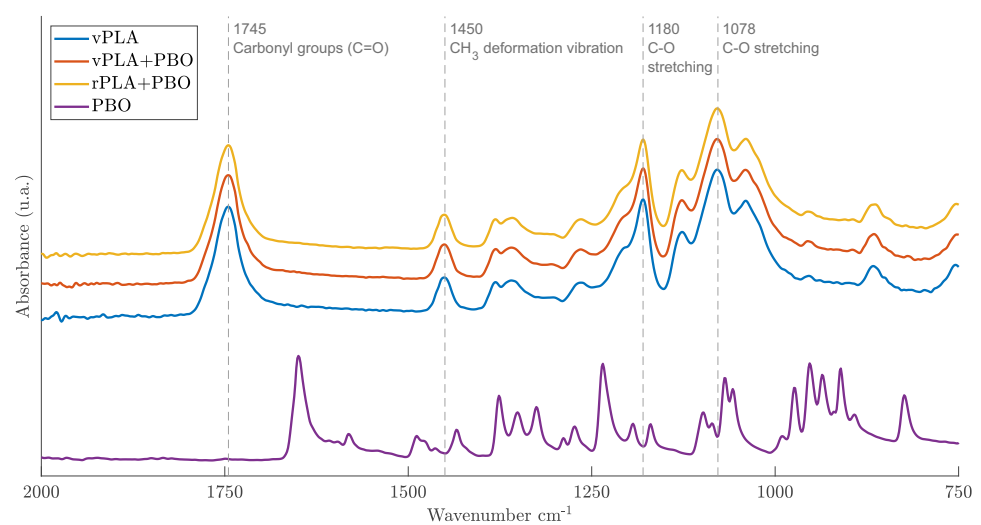


Figure 9. FTIR spectra for virgin PLA (vPLA), chain extender (PBO), virgin PLA mixed in the presence of PBO (vPLA+PBO), and recycled PLA mixed in the presence of PBO (rPLA+PBO).

3.6. Melt Flow Rate

The MFR results (Figure 10) demonstrated that PLA's MFR increased by $\approx 44\%$ after its reprocessing without the chain extender. This behavior can be associated with a viscosity decrease that might have occurred due to the PLA molecular weight decrease, suggesting that the consecutive processing stages caused some extent of molecular degradation [49]. Moreover, the high standard deviation obtained for rPLA formulation indicates that the MFR values between replicates are more spread out, which can be associated with a shape factor of the 3D-printed parts regrind used to perform the tests [50].

After the incorporation of PBO, the MFR value for the virgin PLA was approximately the same, whereas the incorporation of the PBO in the recycled PLA led to an increase in the MFR by $\approx 21\%$, when compared to the neat recycled polymer. These results are in disagreement with several reports from the literature, where the recovery of the molecular weight, due to the reaction between the degraded polymer and the chain extender, was translated into a significant decrease in the MFR [22,46,51,52]. This phenomenon indicates that PBO, instead of reacting with PLA polymeric chains, actually may have acted as a plasticizer that potentiated the sample's fluidity.

Finally, and although the obtained MFR results are not comparable to most of the literature or the manufacturer TDS due to the distinct test conditions, from the experimentation tests it could be concluded that this grade of PLA has a fluidity clearly beyond the theoretical processing window for a general 3D-printing application. However, after performing a parametric optimization of 3D-printer process parameters it is possible to set up the machine to mechanically push the filament at a rate which is compatible to its MFR, therefore assuring the material's printability.

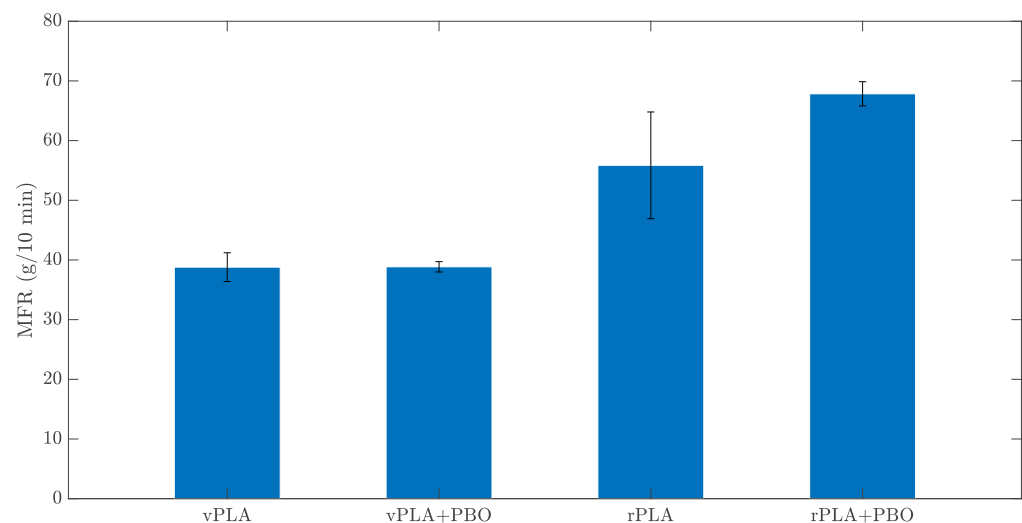


Figure 10. MFR of virgin PLA (vPLA), recycled PLA (rPLA) virgin PLA mixed in the presence of PBO (vPLA+PBO), and recycled PLA mixed in the presence of PBO (rPLA+PBO) at 180 °C and 1.2 kg load.

3.7. Printability Test

The major limitation for the printability of each PLA-based formulation used was the brittle behavior of the material, corroborated by the filament tensile tests, and which contributed to the low success rate of the 3D-printing stage, since the filament was prone to breaking before it could be fed into the 3D printer's nozzle. Moreover, filament spools from the different PLA formulations were not kept at controlled ambient conditions, which could have contributed to a brittle behavior, which became more evident over the course of the experimental work, particularly for the recycled polymer formulations.

From the components that could be completely or partially printed, virgin PLA-based formulations demonstrated the best 3D-printing performance, with no evident signs of

under- or over-extrusion and sufficient structural support to print the $\approx 20^\circ$ overhangs of the regular dodecahedron without helpers (i.e., break away support structures). On the other hand, after mechanical recycling, there was a shift in the ability to process the material through FFF technology. In fact, before chain extension (rPLA), the printability test was not able to be conducted due to the extreme brittleness of the filament. In turn rPLA+PBO allowed to obtain a 3D part, although it showed clear signs of under extrusion associated with segments of filament having inconsistent diameters, below the calculated average. Table 5 presents the data obtained from the qualitative analysis of the print quality with the different PLA-based formulations.

Table 5. Qualitative analysis of the print quality of the formulations of each recycling chain by addressing the success of the print, under- or over-extrusion, presence of voids and bubbles and layer shifts.

Formulation	Description
vPLA	The filament produced with the vPLA formulation was able to be printed, at the specified process parameters; moreover, the resulting components did not show evident signs of under or over extrusion, voids and layer misalignment. However, some inclusions among the deposited beads were detected and the brittle behavior of the material led to a low 3D-printing success rate; a regular dodecahedron and a set of tensile tests for accessing the mechanical performance of this formulation were able to be produced;
rPLA	100% recycled PLA was not able to be printed due to the extreme brittleness of the filament and, therefore, the printability analysis was not able to be conducted;
vPLA+PBO	After chain extension, virgin PLA was able to be printed at the same processes parameters as the vPLA formulation. No evident signs of under or over extrusion, voids and layer misalignment were detected. However, due to the brittle nature of the filament only a partially printed dodecahedron was able to be produced, as well as a set of tensile specimens for accessing the mechanical performance of this formulation;
rPLA+PBO	After chain extension, recycled PLA was able to be printed at the same process parameters as the vPLA formulation; however, evident signs of under- or over-extrusion were detected, as well as the presence of voids and layer misalignment, which were associated with the lower melt strength of this formulation. Moreover, due to embrittlement of the filament over time, it was not possible to produce the set of tensile specimens required for accessing the mechanical performance of this formulation. A regular dodecahedron for the printability test was able to be produced.

3.8. Tensile Performance of 3D-Printed Specimens

Due to printability constraints, it was not possible to produce enough replicates to address the mechanical performance of the recycled PLA-based formulations and, therefore, only the results for vPLA and vPLA+PBO are presented (Figure 11). Moreover, technological limitations regarding the testing equipment did not allow for the calculation of the tensile modulus for the given formulations.

The tensile properties of vPLA after being processed through FFF are significantly lower than those of pristine PLA formulations employed in similar studies available in the literature [7,35,53]. In particular, a decrease in tensile strength (-22.4%) when compared to an injection molding grade PLA used as control material by Grigora et al. in the production of FFF-based specimens is identified [35]. A more evident decrease in tensile strength is further identified when comparing vPLA to extrusion grade PLA processed through FFF (-26.3%) [7], and Fused Particle Fabrication (-37.6%) [53], with the latter being a MEX-AM technology which has been reported to provide a less demanding manufacturing cycle, from the material degradation perspective [53]. These results demonstrate that the processing technology, printing parameters (e.g. toolpath pattern), and the raw material quality highly influence the tensile strength of PLA-based materials. Furthermore, as

the grade of PLA employed in the context of this study has less favorable native tensile performance, its recyclability and further applications are constrained.

Moreover, the obtained results indicate that the incorporation of PBO into the virgin PLA did not affect its native tensile performance, as reflected by the slight increase in the tensile strength (+0.85%) and elongation at break (+7.14%). The steadiness of the mechanical performance parameters between the control and the compatibilized formulation indicated a low interaction between PLA and the PBO, corroborating with the structural analysis and the MFR results.

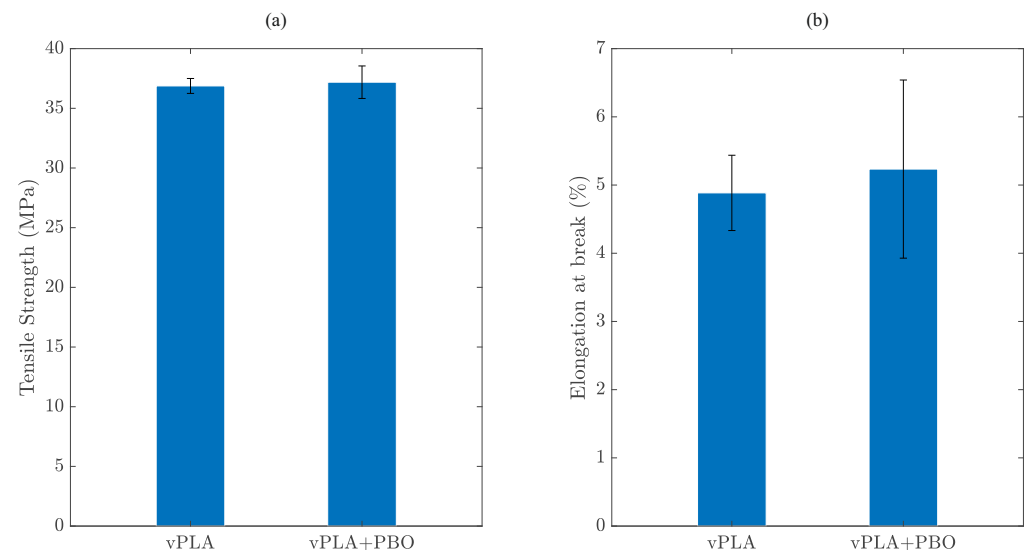


Figure 11. Tensile Strength (a) and Elongation at break (b) of the specimens produced through FFF technology with virgin PLA (vPLA) and virgin PLA mixed in the presence of PBO (vPLA+PBO).

4. Conclusions

The mechanical recycling of PLA decreased its tensile properties and melt strength, as reflected by the decrease in the tensile modulus and tensile strength of the recycled PLA filaments and MFR increase, when compared to its virgin counterpart. After the chain extension with PBO, recycled PLA partially recovered its tensile performance, as reflected by an increase in both the tensile modulus and tensile strength of the specimens, when compared to rPLA. However, PBO did not allow the PLA melt strength to recover. Moreover, the vibrational spectroscopy of neat PLA and compatibilized formulations reflect a low interaction between the polymer and PBO. The compatibilization between the virgin polymer and PBO did not significantly affect the mechanical performance and melt strength of the material, but did for the originating peninsula-like layers and some extent of fibrils in the material. Optical measurements reflected a noticeable discoloration, reflected by an yellowing of the virgin polymer after the PBO incorporation.

Regarding the processability of the material, filaments with consistent diameter were able to be produced with all the formulations obtained in each recycling chain. A linear mass density consistency analysis was conducted by comparing the linear mass density computed through the ratio between the filament weight and the filament length and a theoretical counterpart based on the PLA density as stated on the manufacturer's TDS. This analysis allowed us to understand that the vPLA filament was the most contaminated formulation, a result which was further corroborated by the surface morphology observations. These inclusions were attributed to the consumption of certain additives incorporated in the supplied PLA formulation (e.g., antioxidants). For accessing the printability of the material, different components were produced through an open-source 3D printer. It was possible to print 3D parts with all the formulations of each recycling chain, except of the 100% recycled PLA. The brittle nature of the material represented the major constraint

for either virgin polymer or compatibilized formulations, since the filament was prone to break in the extruder which led to a very low success rate in the 3D-printing stage. In this context, it was not possible to establish a closed-loop recycling scheme by employing the developed methodology nor with the multi-processing approach to the virgin PLA or the virgin PLA/PBO and recycle-recovered PLA formulations.

The incorporation of the chain extender as an upgrading strategy for both virgin and recycled PLA led to inconclusive results, since on the one hand recycled PLA after the chain extension seems to partially recover its mechanical performance, as reflected in the filament tensile tests, but, on the other hand, the MFR results, which provide an insight on the rheological properties of the material and, therefore, of the molecular weight of the polymer, demonstrate an increasing trend where a significant decrease was expected. In this context, further characterization of the chain extender should be considered in order to better understand how it reacts with the PLA and, therefore, enabling the definition of the optimum CE concentration which favors the PLA chain extension.

Author Contributions: Conceptualization, T.E.P.G., I.G. and V.N.; Formal analysis, C.C. and I.G.; Funding acquisition, V.N.; Investigation, Carlos Correia, T.E.P.G., I.G. and V.N.; Methodology, C.C., T.E.P.G., I.G. and V.N.; Supervision, I.G. and V.N.; Validation, I.G. and V.N.; Writing—original draft, C.C. and T.E.P.G.; Writing—review and editing, I.G. and V.N. All authors have read and agreed to the published version of the manuscript.

Funding: This research was funded by University of Aveiro, FCT/MCTES through the financial support of TEMA research unit (FCT Ref. UIDB/00481/2020 & UIDP/00481/2020) and CICECO-Aveiro Institute of Materials (FCT Ref. UIDB/50011/2020 & UIDP/50011/2020). The authors also acknowledge FCT – Fundação para a Ciência e a Tecnologia, I.P. for the PhD grants ref. SFRH/BD/143429/2019 (TEPG). FCT is also thanked for the Individual Call to Scientific Employment Stimulus (IG, FCT ref. CEECIND/00430/2017).

Data Availability Statement: The data that support the findings of this study are available from the corresponding authors upon reasonable request.

Conflicts of Interest: The authors declare no conflict of interest. The funders had no role in the design of the study; in the collection, analyses, or interpretation of data; in the writing of the manuscript, or in the decision to publish the results.

References

1. Geyer, R.; Jambeck, J.R.; Law, K.L. Production, use, and fate of all plastics ever made. *Sci. Adv.* **2017**, *3*, 25–29. [[CrossRef](#)] [[PubMed](#)]
2. Badia, J.D.; Ribes-Greus, A. Mechanical recycling of polylactide, upgrading trends and combination of valorization techniques. *Eur. Polym. J.* **2016**, *84*, 22–39. [[CrossRef](#)]
3. Badia, J.D.; Óscar Gil-Castell; Teruel-Juanes, R.; Ribes-Greus, A. Recycling of Polylactide. In *Encyclopedia of Renewable and Sustainable Materials*; Elsevier BV: Amsterdam, The Netherlands, 2020; pp. 282–295. [[CrossRef](#)]
4. Vilaplana, F.; Karlsson, S. Quality concepts for the improved use of recycled polymeric materials: A review. *Macromol. Mater. Eng.* **2008**, *293*, 274–297. [[CrossRef](#)]
5. Pillin, I.; Montrelay, N.; Bourmaud, A.; Grohens, Y. Effect of thermo-mechanical cycles on the physico-chemical properties of poly(lactic acid). *Polym. Degrad. Stab.* **2008**, *93*, 321–328. [[CrossRef](#)]
6. Zenkiewicz, M.; Richert, J.; Rytlewski, P.; Moraczewski, K.; Stepczyńska, M.; Karasiewicz, T. Characterisation of multi-extruded poly(lactic acid). *Polym. Test.* **2009**, *28*, 412–418. [[CrossRef](#)]
7. Sanchez, F.A.C.; Boudaoud, H.; Hoppe, S.; Camargo, M. Polymer recycling in an open-source additive manufacturing context: Mechanical issues. *Addit. Manuf.* **2017**, *17*, 87–105. [[CrossRef](#)]
8. Ragaert, K.; Delva, L.; Geem, K.V. Mechanical and chemical recycling of solid plastic waste. *Waste Manag.* **2017**, *69*, 24–58. [[CrossRef](#)]
9. Brüster, B.; Addiego, F.; Hassouna, F.; Ruch, D.; Raquez, J.M.; Dubois, P. Thermo-mechanical degradation of plasticized poly(lactide) after multiple reprocessing to simulate recycling: Multi-scale analysis and underlying mechanisms. *Polym. Degrad. Stab.* **2016**, *131*, 132–144. [[CrossRef](#)]
10. Botta, L.; Scaffaro, R.; Suter, F.; Mistretta, M.C. Reprocessing of PLA/graphene nanoplatelets nanocomposites. *Polymers* **2018**, *10*, 18. [[CrossRef](#)]
11. Preparation and recycling of plasticized PLA. *Macromol. Mater. Eng.* **2011**, *296*, 141–150. [[CrossRef](#)]

12. Badia, J.D.; Strömberg, E.; Karlsson, S.; Ribes-Greus, A. Material valorisation of amorphous polylactide. Influence of thermo-mechanical degradation on the morphology, segmental dynamics, thermal and mechanical performance. *Polym. Degrad. Stab.* **2012**, *97*, 670–678. [[CrossRef](#)]
13. Cuadri, A.A.; Martín-Alfonso, J.E. Thermal, thermo-oxidative and thermomechanical degradation of PLA: A comparative study based on rheological, chemical and thermal properties. *Polym. Degrad. Stab.* **2018**, *150*, 37–45. [[CrossRef](#)]
14. Agüero, A.; del Carmen Morcillo, M.; Quiles-Carrillo, L.; Balart, R.; Boronat, T.; Lascano, D.; Torres-Giner, S.; Fenollar, O. Study of the influence of the reprocessing cycles on the final properties of polylactide pieces obtained by injection molding. *Polymers* **2019**, *11*, 1908. [[CrossRef](#)] [[PubMed](#)]
15. Tuna, B.; Ozkoc, G. Effects of Diisocyanate and Polymeric Epoxidized Chain Extenders on the Properties of Recycled Poly(Lactic Acid). *J. Polym. Environ.* **2017**, *25*, 983–993. [[CrossRef](#)]
16. BASF. *Polymeric Chain Extenders Joncry ADR-4368 Data Sheet*; Technical Report; BASF Corporation: Florham Park, NJ, USA, 2008.
17. Khankrua, R.; Pivsa-Art, S.; Hiroyuki, H.; Suttiruengwong, S. Effect of chain extenders on thermal and mechanical properties of poly(lactic acid) at high processing temperatures: Potential application in PLA/Polyamide 6 blend. *Polym. Degrad. Stab.* **2014**, *108*, 232–240. [[CrossRef](#)]
18. Meng, X.; Shi, G.; Chen, W.; Wu, C.; Xin, Z.; Han, T.; Shi, Y. Structure effect of phosphite on the chain extension in PLA. *Polym. Degrad. Stab.* **2015**, *120*, 283–289. [[CrossRef](#)]
19. Meng, X.; Shi, G.; Wu, C.; Chen, W.; Xin, Z.; Shi, Y.; Sheng, Y. Chain extension and oxidation stabilization of Triphenyl Phosphite (TPP) in PLA. *Polym. Degrad. Stab.* **2016**, *124*, 112–118. [[CrossRef](#)]
20. Han, T.; Xin, Z.; Shi, Y.; Zhao, S.; Meng, X.; Xu, H.; Zhou, S. Control of thermal degradation of poly(lactic acid) using functional polysilsesquioxane microspheres as chain extenders. *J. Appl. Polym. Sci.* **2015**, *132*, 1–11. [[CrossRef](#)]
21. Ramírez-Herrera, C.A.; Flores-Vela, A.I.; Torres-Huerta, A.M.; Domínguez-Crespo, M.A.; Palma-Ramírez, D. PLA degradation pathway obtained from direct polycondensation of 2-hydroxypropanoic acid using different chain extenders. *J. Mater. Sci.* **2018**, *53*, 10846–10871. [[CrossRef](#)]
22. Liu, W.; Li, H.; Wang, X.; Du, Z.; Zhang, C. Effect of chain extension on the rheological property and thermal behaviour of poly(lactic acid) foams. *Cell. Polym.* **2013**, *32*, 343–368. [[CrossRef](#)]
23. Alturkestany, M.T.; Panchal, V.; Thompson, M.R. Improved part strength for the fused deposition 3D printing technique by chemical modification of polylactic acid. *Polym. Eng. Sci.* **2019**, *59*, E59–E64. [[CrossRef](#)]
24. Fuentes, M.A.V.; Thakur, S.; Wu, F.; Misra, M.; Gregori, S.; Mohanty, A.K. Study on the 3D printability of poly(3-hydroxybutyrate-co-3-hydroxyvalerate)/poly(lactic acid) blends with chain extender using fused filament fabrication. *Sci. Rep.* **2020**, *10*, 1–12. [[CrossRef](#)]
25. *Additive Manufacturing—General Principles—Terminology*; Standard, International Organization for Standardization: Geneva, Switzerland, 2015.
26. Brian; Redwood, B.; Schoffer, F.G. *The 3D Printing Handbook*; Coers & Roest: Arnhem, The Netherlands, 2013; p. 2013.
27. Jordan, J. *3D Printing*; The MIT Press: Cambridge, MA, USA, 2018; p. 238.
28. RePET. About | RE PET 3D. Available online: <https://re-pet3d.com/about/> (accessed on 1 July 2021).
29. Filamentive—Recycled 3D Printing Filament UK. Available online: <https://www.filamentive.com/about-filamentive-recycled-filament/> (accessed on 1 July 2021).
30. Reflow. About—REFLOW. Available online: <https://reflowproject.eu/about/> (accessed on 1 July 2021).
31. Azevedo, J. Novo Filamento 3D Produzido a Partir de Desperdícios de Plástico dos Makers | TUCAB. Available online: <https://bit.ly/2VlaUqE>. (accessed on 1 July 2021).
32. Gomes, T. Utilização de matéria prima secundária polimérica para aplicações em fabrico aditivo. Master's Thesis, Universidade de Aveiro, Aveiro, Portugal, 2013.
33. Sanchez, F.A.C.; Boudaoud, H.; Camargo, M.; Pearce, J.M. Plastic recycling in additive manufacturing: A systematic literature review and opportunities for the circular economy. *J. Clean. Prod.* **2020**, *264*, 121602. [[CrossRef](#)]
34. Moreno, E.; Beltrán, F.R.; Arrieta, M.; Gaspar, G.; Muneta, M.L.M.; Carrasco-Gallego, R.; Yañez, S.; Hidalgo, D.; Orden, M.U.D.L.; Urreaga, J.M. Technical Evaluation of Mechanical Recycling of PLA 3D Printing Wastes. *Proceedings* **2020**, *69*, 19.
35. Grigora, M.E.; Terzopoulou, Z.; Tsongas, K.; Klonos, P.; Kalafatakis, N.; Bikiaris, D.N.; Kyritsis, A.; Tzetzis, D. Influence of reactive chain extension on the properties of 3d printed poly(Lactic acid) constructs. *Polymers* **2021**, *13*, 1381. [[CrossRef](#)]
36. Marec, P.E.L.; Ferry, L.; Quantin, J.C.; Benezet, J.C.; Bonfils, F.; Guilbert, S.; Bergeret, A. Influence of melt processing conditions on poly(lactic acid) degradation: Molar mass distribution and crystallization. *Polym. Degrad. Stab.* **2014**, *110*, 353–363. [[CrossRef](#)]
37. GmbH, W.T. Compact—Wanner Technik GmbH. Available online: <https://www.wanner-technik.de/en/granulators/compact/> (accessed on 22 June 2021).
38. *Tips and Tricks for Successful Tensile Testing: Stretching the Boundaries in Your Lab*; Technical report; Stable Micro Systems: Surrey, UK, 2015.
39. *Plastics—Determination of tensile properties—Part 2: Test Conditions for Moulding and Extrusion Plastics*; Standard, International Organization for Standardization: Geneva, Switzerland, 2014.
40. Gonçalves, I.; Lopes, J.; Barra, A.; Hernández, D.; Nunes, C.; Kapusniak, K.; Kapusniak, J.; Evtyugin, D.V.; da Silva, J.A.L.; Ferreira, P.; et al. Tailoring the surface properties and flexibility of starch-based films using oil and waxes recovered from potato chips byproducts. *Int. J. Biol. Macromol.* **2020**, *163*, 251–259. [[CrossRef](#)]

41. *Plastics—Differential Scanning Calorimetry (DSC)—Part 1: General Principles (ISO 11357-1:2009)*; Standard, International Organization for Standardization: Brussels, Switzerland, 2009.
42. Beltrán, F.R.; Lorenzo, V.; de la Orden, M.U.; Martínez-Urreaga, J. Effect of different mechanical recycling processes on the hydrolytic degradation of poly(L-lactic acid). *Polym. Degrad. Stab.* **2016**, *133*, 339–348. [[CrossRef](#)]
43. Petchwattana, N.; Channuan, W.; Naknaen, P.; Narupai, B. 3D printing filaments prepared from modified poly(lactic acid)/teak wood flour composites: An investigation on the particle size effects and silane coupling agent compatibilisation. *J. Phys. Sci.* **2019**, *30*, 169–188. [[CrossRef](#)]
44. Costa, A. Nanocompósitos de matriz polimérica para impressão 3D. Master's Thesis, Universidade de Aveiro, Aveiro, Portugal, 2016.
45. Zhao, X.G.; Hwang, K.J.; Lee, D.; Kim, T.; Kim, N. Enhanced mechanical properties of self-polymerized polydopamine-coated recycled PLA filament used in 3D printing. *Appl. Surf. Sci.* **2018**, *441*, 381–387. [[CrossRef](#)]
46. Barletta, M.; Aversa, C.; Puopolo, M. Recycling of PLA-based bioplastics: The role of chain-extenders in twin-screw extrusion compounding and cast extrusion of sheets. *J. Appl. Polym. Sci.* **2020**, *137*, 49292. [[CrossRef](#)]
47. Rasselet, D.; Caro-Bretelle, A.S.; Taguet, A.; Lopez-Cuesta, J.M. Reactive compatibilization of PLA/PA11 blends and their application in additive manufacturing. *Materials* **2019**, *12*, 485. [[CrossRef](#)] [[PubMed](#)]
48. Gonçalves, C.M.B.; Coutinho, J.A.P.; Marrucho, I.M. *8 Optical Properties*; John Wiley & Sons, Inc.: Hoboken, NJ, USA, 2010; pp. 97–112.
49. Carrasco, F.; Pagès, P.; Gámez-Pérez, J.; Santana, O.O.; MasPOCH, M.L. Processing of poly(lactic acid): Characterization of chemical structure, thermal stability and mechanical properties. *Polym. Degrad. Stab.* **2010**, *95*, 116–125. [[CrossRef](#)]
50. Singh, N.; Singh, R.; Ahuja, I.P. Recycling of polymer waste with SiC/Al₂O₃ reinforcement for rapid tooling applications. *Mater. Today Commun.* **2018**, *15*, 124–127. [[CrossRef](#)]
51. Ghalia, M.A.; Dahman, Y. Investigating the effect of multi-functional chain extenders on PLA/PEG copolymer properties. *Int. J. Biol. Macromol.* **2017**, *95*, 494–504. [[CrossRef](#)]
52. Baimark, Y.; Srihanam, P. Influence of chain extender on thermal properties and melt flow index of stereocomplex PLA. *Polym. Test.* **2015**, *45*, 52–57. [[CrossRef](#)]
53. Alexandre, A.; Sanchez, F.C.; Boudaoud, H.; Camargo, M.; Pearce, J. Mechanical Properties of Direct Waste Printing of Polylactic Acid with Universal Pellets Extruder: Comparison to Fused Filament Fabrication on Open-Source Desktop Three-Dimensional Printers. *3D Print. Addit. Manuf.* **2020**, *7*, 237–247. [[CrossRef](#)]